# Fluid and Structural Dynamic Design Considerations of the HYLIFE Nozzle Plate

J.H. Pitts
*University of California, Lawrence Livermore National Laboratory, P.O. Box 5508, Livermore, California 94550, U.S.A.*

I.U. Ojalvo
*Perkin-Elmer, Optical Technology Division, 100 Wooster Heights Road, Danbury, Connecticut 06810, U.S.A.*

I.U. Ojalvo

Employed by Grumman Aerospace Corporation, Bethpage, New York, at the time this work was completed.

SUMMARY

The basic concept of the High Yield Lithium Injection Fusion Energy (HYLIFE) reaction chamber [1] involves a falling liquid-metal (lithium) jet array that absorbs 90% of the energy released from inertial confinement fusion reactions. The key element of the chamber that produces the jet array is the nozzle plate. This paper describes the design and analysis of a nozzle plate which can withstand the structural loads and permit the fluid jet array to be reestablished for a 1-Hz fusion reaction frequency.

The shape of the nozzle plate and jet array is dictated by considerations of fluid dynamics and neutron-shielding. A vertical jet array, rather than a single annulus, is used because this design enhances fluid momentum interchange and dissipation of the kinetic energy that occurs when the jets disassemble. Less net outward-directed momentum results than with a single liquid annular flow configuration, thus producing lower stresses in the structural components.

The lithium head is established to ensure that the velocity of the free jets leaving the nozzle plate is sufficient for them to reestablish themselves between fusion reactions. The jet channels have a constant cross section, arranged in a pattern that maximizes shielding uniformity. An annular weir flow over the plate's central hole provides shielding for the inner areas of the plate. Geometric perturbations at discrete locations around the circumference of the weir are intentionally introduced so that the weir flow breaks up into jets before it reaches the reaction chamber midplane.

A variable-property thick annular wedge was used to structurally model the nozzle plate. The static loads imposed were those due to the head of lithium, drag of the fluid as it entered the nozzle plate and the weight of the plate itself. Dynamic loads resulted from neutron-induced pressure above the plate, and lithium gas pressure and liquid impact pressures below the nozzle plate. An approximate Rayleigh-Ritz procedure was used in conjunction with a finite element program to obtain the stress components. It was found that the design thickness was dictated by the plate static stresses in conjunction with appropriate design stress concentration factors and fatigue considerations.

Work partially performed under the auspices of the U.S. Department of Energy by Lawrence Livermore Laboratory under contract number W-7405-ENG-48.

## 1. Introduction

A D-T fuel pellet is injected once each second into the center of the HYLIFE reaction chamber and laser drivers initiate the fusion reactions. The circulation system used to transfer energy from the reaction chamber to the turbine unit consists of 16 lithium primary loops, four sodium intermediate heat-exchanger loops and four superheated steam secondary loops.

The nozzle plate (shown in Fig. 1) is a 0.5 m thick, 5 m radius circular disk that is simply supported at its outside edge by a series of gussets attached to the first structural wall. It is constructed of 33 mm thick, extruded angle plates welded together. The part of the plate through which the jet array passes contains constant-cross-section vertical channels. The structure of the outer portion is similar, except for the bottom and top, which are closed by flat plates that prevent flow-through of lithium and give additional strength. Some lithium circulation does occur in this outer region, with the result that the maximum metal temperature remains below 800 K. This circulation flow can be discharged to cool the first structural wall, graphite reflector, and vacuum vessel, as well. A central hole allows rapid equalization of pressure from each fusion reaction on the top and bottom of the nozzle plate. An annular lithium weir flow exists over the edge of the central hole so that the inner areas of the nozzle plate are protected from x rays and neutrons. Intentional geometric perturbations in the weir area are shown schematically in Fig. 1. The optimum shape of these perturbations would be established empirically to offer maximum shielding and yet force the weir to break up into jets before reaching the reaction chamber midplane.

The shape of the vertical channels is generally rectangular. Radial webs between the channels are located so that a line of sight from the location of the fusion reactions to the first structural wall passes through four or more jets. The flow separates at the entrance of each channel, and then falls under the influence of gravity through the reaction chamber. Hence, fluid flow forces are decoupled from the structural loading considerations that dictate the nozzle plate thickness. There are additional jets (not shown in Fig. 1) that shield the laser-beam and pellet-injection regions.

A major advantage of this nozzle plate design is its adaptability. The pattern of the jet array will undoubtedly change as more analytical results and experimental data become available. Any reasonable jet pattern can be accommodated with minor revisions to the nozzle plate inner-jet-flow region. The plate thickness can thus be adjusted to assure adequate structural performance. In fact, changes in the jet pattern can be incorporated with only secondary difficulty, even after the reaction chamber has been operated, by lifting the nozzle plate out of the chamber and replacing it with an alternate version.

## 2. Fluid Mechanics Considerations.

The basic design of the nozzle plate was established to yield a jet array (including the weir flow) that has a 0.55 m inner radius and a 2.5 m radial thickness at the reaction chamber vertical midplane. The packing fraction at the midplane is $\sim$ 35%, which results in $\sim$ 0.8 m effective radial thickness for shielding purposes. Ninety percent of the energy from the fusion reactions is deposited directly in the jet array and automatically flows out of the reaction chamber. This reduces the heat generation in metal components by an order of magnitude and eases potential cooling problems. The reduced flux reaching the

metal walls plus the choice of 2¼ Cr-1 Mo steel produce induced activation in metal components that is lower by a factor of 100 than that in a Tokamak with 316-stainless steel walls. This reduced activity could be a major environmental issue resulting in the selection of HYLIFE over other types of fusion reactions chambers. Furthermore, this reduced flux allows the design of structural members that can last the entire 30-year lifetime projected for the reaction chamber without exceeding the allowable 160-dpa radiation damage limit [2]. A larger inner radius could have been chosen, but this would require a larger flow rate and pumping power for the same shielding protection. A smaller inner radius is not permissible because this would result in excessive stresses in the first structural wall [3].

A 5.5 m/s downward jet velocity at the bottom of the nozzle plate was selected so that the jets are reestablished throughout the chamber before the next fusion reaction occurs 1 s later. In actuality, the jets only need to be reestablished in the upper 7 or 8 m of the chamber prior to the next fusion reaction because the lower portion contains a lithium pool. This conservatism allows for additional disruptions of the jets which have not yet been fully analyzed (e.g., effects of gas pressure below the nozzle plate on the initial jet velocity in the first ten milliseconds, following a fusion reaction). The initial velocity dictates the head of lithium that must be present above the nozzle plate. Under ideal conditions, this head would be equivalent to the dynamic head. The static head of fluid above the plate was selected to give the desired 5.5 m/s at the bottom of the nozzle plate. The actual magnitude of the head of lithium will need to be established empirically because of the complex flow pattern that exists in the upper pool. The entrances to the jets are rounded to minimize losses and contraction of the jets. Because jet-area contraction coefficients of unity are typical for such entrances, the jet would have the same dimensions as the channel at the top of the nozzle plate.

The thickness of each jet decreases as it falls. Conservation of energy and the continuity relationship can be used to show that a radial jet thickness of 0.3 m at the nozzle plate becomes 0.15 to 0.2 m at the midplane, depending on the aspect ratio of the jet. Radial webs in the nozzle plate that separate the flow channels are positioned so that a ray from the fusion reaction to the first structural wall passes through at least four of the six rows of jets. Additional curved jets are located around the beam-port areas, forming an arched pattern to shield their metal portions.

Experiments [4] in progress at the University of California at Davis show that rectangular-shaped jets oscillate in time with the major axis becoming the minor axis (and vice versa). These experiments use water and relatively small jets. Preliminary theoretical and experimental results suggest that, with the large lithium jets present in HYLIFE, no appreciable variation in the jet axis will occur before the lithium reaches the bottom of the reaction chamber.

Breakup of the jets into droplets has also been found not to exist under HYLIFE conditions. Hoffman [2,4] and Kusui [5] have shown that the "breakup length" is related by

$$L/D = 55 + 1.085(N_W)^{0.5}, \qquad (1)$$

where L is the "breakup length", D is the characteristic diameter of the jet, and $N_W$ is

the Weber number. For 0.3 m thick lithium jets having an initial velocity of 4.5 m/s, the breakup length is 45 m. This is well beyond the 8 to 10 m working length of the reaction chamber, and it indicates the jets will remain intact.

Dynamic loads are imposed on the nozzle plate following each fusion reaction [6]. A downward pressure induced by the sudden deposition of neutron energy in the upper lithium pool during the first 300 μs varies with radius. Its peak magnitude is 1.5 MPa. In addition, short-ranged x rays and pellet debris vaporize and superheat lithium in the central area of the reaction chamber, which results in an upward pressure on the nozzle plate. This upward pressure also varies with space and time, with a peak magnitude of 3 MPa. Additional static pressure loads, up to 200 kPa, result from the dead weight of the nozzle plate itself and the liquid lithium. Effects of the steady lithium fluid acceleration from the upper lithium pool into the flow channels was considered when determining these static loads.

3. Structural Dynamic Considerations.

The HEX three-dimensional element of the PLANS finite-element computer program was used to model a six-degree wedge of the nozzle plate [7,8,9]. Orthotropic properties, which vary with radius, were used for 50 eight-noded, six-sided, isoparametric elements used in the study. These properties were based upon local material thickness ratios in the various element directions.

A full, standard dynamic solution by either normal-mode or transient-response methods was circumvented by using an approximate modal approach. The method starts with the governing finite-element dynamic plate equations

$$[M]\ \{\ddot{\delta}\} + [K]\ \{\delta\} = \{F(t)\} \tag{2}$$

where [M] and [K] are the plate mass and stiffness matrices, respectively, $\{\delta\}$ are the time-dependent nodal displacements, and {F} are the transient nodal forces. The mass and stiffness matrices are generated by a standard finite element computer program once the appropriate geometry and material properties are input.

The adopted solution procedure is as follows: The forcing function {F} may be decomposed [8] into a series of products of spatial, $\{P_i\}$, and temporal, $f_i(t)$, functions

$$\{F\} \sim \sum_i \{P_i\}\ f_i(t) \tag{3}$$

Approximate solutions of the form

$$\{\delta\} \sim \sum_i \{\delta_i\}\ X_i(t) \tag{4}$$

are sought, where $\{\delta_i\}$ are assumed modes that satisfy the statical equations, i.e.,

$$[K]\ \{\delta_i\} = \{P_i\},\ i=1,2,\ldots \tag{5}$$

The use of statical solutions assumes that the dynamic stresses and deflections may be

formed as a linear combination of these distributions, where the dynamic stresses, $\{\sigma(t)\}$, are given by the stress matrix, [S],

$$\{\sigma(t)\} = \sum \{\sigma_i\} = [S] \sum \{\delta_i\} X_i(t) \tag{6}$$

Substitution of Eqs. (3), (4), and (5) into Eq. (2) and equating in terms of equal i yields

$$[M] \{\delta_i\} \ddot{X}_i + [K] \{\delta_i\} X_i \sim \{P_i\} f_i = [K] \{\delta_i\} f_i, \quad i=1,2,... \tag{7}$$

Multiplying Eq. (7) by $\{\delta_i\}^T$ and defining $\omega_{Ri}^2$ as the Rayleigh quotient gives the transpose of the nodal displacement vector:

$$\omega_{Ri}^2 = \frac{\{\delta_i\}^T [K] \{\delta_i\}}{\{\delta_i\}^T [M] \{\delta_i\}} = \frac{\{P\}^T \{\delta_i\}}{\{\delta_i\}^T [M] \{\delta_i\}}, \quad i=1,2,... \tag{8}$$

and dividing Eq. (7) by $\{\delta_i\}^T [M]\{\delta_i\}$ yields

$$\ddot{X}_i + \omega_{Ri}^2 X_i = \omega_{Ri}^2 f_i(t), \quad i=1,2,... \tag{9}$$

Starting with the dynamic forcing functions, statical-mode shapes $\{\delta_i\}$ and Rayleigh quotients $\omega_{Ri}^2$ were obtained through solution of Eqs. (5) and (8), respectively. Then, Eq. (9) was solved by a computerized numerical-integration scheme subject to the quiescent initial conditions

$$X_i(0) = 0 \tag{10a}$$
$$\dot{X}_i(0) = 0 \tag{10b}$$

and the results were combined as indicated by Eq. (4) to yield an approximation for $\{\delta(t)\}$ and the stresses.

### 3.1 Stress Scaling Laws

Because basic parameters of the present nozzle-plate configuration will change as the conceptual design develops, it would be convenient to identify the influence that such changes would have upon primary stresses. As may be seen from Eq. (4), (5), and (9), the dynamic plate stresses ($\sigma_d$) are proportional to the Rayleigh quotient $\omega_R^2$, and the modal stresses, ($\sigma_a$) associated with the "assumed" trial mode shape, i.e.

$$\sigma_d \sim \omega_{Ri}^2 \sigma_2 \tag{11}$$

where

$$\sigma_a \sim q_{dynamic} \left(\frac{a}{h}\right)^2$$

In Eq. (12), $q_{dynamic}$ is a measurement of the dynamic loading intensity, h is the plate thickness, and a is the plate outer radius.

For a given plate design

$$\omega_{Ri}^2 \sim \frac{Eh^2}{\rho a^4} \tag{13}$$

where E is the effective stiffness modulus of the plate material, and $\rho$ is the mass density.

The static stresses ($\sigma_s$), however, depend primarily upon the loading parameter ($q_s$) and the geometric parameters a and h as follows:

$$\sigma_s \sim q_s \left(\frac{a}{h}\right)^2 \tag{14}$$

Therefore, increasing the outer plate radius from a to a' will have the effect of increasing the static stresses in the ratio of $(a'/a)^2$, while decreasing the Rayleigh quotient in the ratio $(a/a')^4$. This reduction in $\omega_R^2$ would result in a decrease in $\sigma_d$ by $(a/a')^2$, since $\sigma_a$ (see Eq. 12) will increase in the ratio $(a'/a)^2$.

Similarly, an increase in h to h' will cause $\sigma_a$ and $\sigma_s$ to decrease in the ratio $(h/h')^2$. However, it will leave $\sigma_d$ unchanged, since the decrease in $\sigma$ is offset by a corresponding increase in $\omega_R^2$. It should be noted that if the change in h to h' increases $q_{static}$, this should be accounted for as well when computing $\sigma_s$.

### 3.2 Results

Results were generated for a nozzle plate of slightly different dimensions than those described here; They were adjusted by use of the stress-scaling laws. A peak static stress of 60 MPa was obtained at the inner radius near the bottom of the nozzle plate as, shown in Fig. 2. Circumferential ($\theta$ direction) static stresses near the top are essentially the negative of those shown. The absolute values of radial and axial stresses (r and z directions) on the top surface are equal to, or less than, those shown. The peak dynamic stress of 10 MPa having a period of about 20 ms is reached at the top and bottom surfaces of the inner radius. This dynamic stress includes the effect of the nonhomogeneous reduced area in the plate.

Static and dynamic peaks both occurred at the same location on the nozzle plate (i.e., at the inner radius of the plate, near the top and bottom surface), and both were circumferential components of stress. The spatial stress distributions shown in Fig. 2 are for a uniform pressure distribution, but all the loadings used gave similarly distributed stresses. In fact, all the trial modes yielded Rayleigh quotient frequencies of around 60 Hz.

A nozzle-plate thickness other than 0.5 m would have resulted in different static stress levels only. (Recall that the dynamic stress magnitudes are independent of nozzle-plate thickness.) The thickness of 0.5 m was selected because of fatigue crack growth considerations. The resulting static stress of 60 MPa coupled with a fluctuating dynamic stress of $\pm$ 10 MPa yields an allowable initial crack length of about 20 mm. This value can be easily detected by ultrasonic techniques. A nozzle plate thickness less than 0.5 m would have resulted in increased static stresses and hence, a marginal ability to detect flaws in the welded areas of the nozzle plate.

## References


[1] PITTS, J., HOVINGH, J., MEIER, W. R., MONSLER, M. J., POWELL, E. G., and WALKER, P. E., "Potential Design Modifications for the High Yield Lithium Injection Fusion Energy (HYLIFE) Reaction Chamber," Proc. 8th Symp. Eng. Prob. Fusion Research, San Francisco, Calif. (Nov. 13-16, 1979).

[2] Laser Program Annual Report-1978, Lawrence Livermore National Laboratory, Livermore, Calif., Sec. 9 and, in particular, pp. 9-18 and 9-21. (1979)

[3] Laser Program Annual Report-1979, Lawrence Livermore National Laboratory, Livermore, Calif., Sec. 8. and, in particular, pp. 8-57 to 8-65. (1980)

[4] HOFFMAN, M., private communication, U. C. Davis (April 1980).

[5] KUSUI, T., "Liquid Jet Flow into Still Gas," Bulletin, Japan Society of Mechanical Engineers, 11, 1084ff (1968).

[6] BLINK, J., Lawrence Livermore National Laboratory, private communication, (January 1980).

[7] PIFKO, A. et al., PLANS-A Finite Element Program for the Nonlinear Analysis of Structures, Grumman Aerospace Corp., Bethpage, N.Y., RM-633 (May 1972).

[8] Grumman Aerospace Corporation, Inertial Confinement Fusion Research and Development Studies, Final Report to the Lawrence Livermore National Laboratory, Purchase Order 6419309, UCRL-15292 (August 1980).

[9] LEVY, A., A Three-Dimensional Variable Node Isoparametric Solid Element, Grumman Aerospace Corp., Bethpage, N.Y., RM-587 (July 1979).

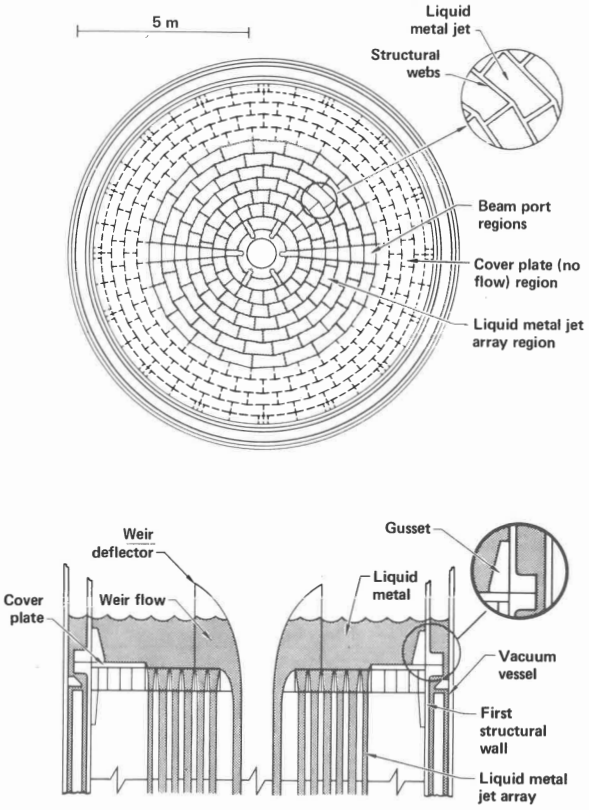


1. Elevation and plan views of the HYLIFE nozzle plate.

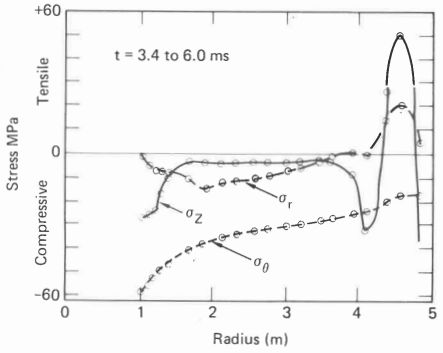


2. Static stresses near the bottom surface.